

## ELECTRONIC SUPPLEMENTARY INFORMATION

# Structural specific of light-induced metastable state in copper(II)-nitroxide molecular magnets

*Irina Yu. Barskaya,<sup>a,b</sup> Sergey L. Veber,<sup>a,b,\*</sup> Sergey V. Fokin,<sup>a</sup> Evgeniy V. Tretyakov,<sup>a,b,c</sup>  
Victor I. Ovcharenko,<sup>a</sup> Elena G. Bagryanskaya,<sup>b,c</sup> Matvey V. Fedin<sup>a,b,\*</sup>*

<sup>a</sup> International Tomography Center SB RAS, Institutskaya str. 3a, 630090, Novosibirsk, Russia

<sup>b</sup> Novosibirsk State University, Pirogova str.2, 630090, Novosibirsk, Russia

<sup>c</sup> N.N. Vorozhtsov Novosibirsk Institute of Organic Chemistry SB RAS, Pr. Lavrentjeva 9,  
630090, Novosibirsk, Russia

## AUTHOR INFORMATION

### Corresponding Authors

[sergey.veber@tomo.nsc.ru](mailto:sergey.veber@tomo.nsc.ru); [mfedin@tomo.nsc.ru](mailto:mfedin@tomo.nsc.ru)

## I. EXPERIMENTAL DETAILS

(a) Preparation of the samples. The studied compounds  $\text{Cu}(\text{hfac})_2\text{L}^{\text{Pr}}$ ,  $\text{Cu}(\text{hfac})_2\text{L}^{\text{i-Pr}}$  and  $\text{Cu}(\text{hfac})_2\text{L}^{\text{Me}}$  have been synthesized according to the developed procedures;<sup>S1,S2</sup> their physicochemical properties were previously characterized by X-ray, SQUID, EPR.<sup>S3-S7</sup> Usual pelleting technique was applied for mid-FTIR experiments (Figure 3): 1–2 mg of studied compound was ground and then mixed with 140 mg of KBr powder; the mixture was pressed in vacuo at room temperature using ≈5 ton pressure applied for 5 minutes. Although the compression procedure leads to partial suppression of magnetostructural transition (that becomes smoothed and lagged), its manifestations in FTIR spectra were found similar in both single crystals and pellets.<sup>S8</sup> Figure 4 used thin single crystals of  $\text{Cu}(\text{hfac})_2\text{L}^{\text{Pr}}$  and  $\text{Cu}(\text{hfac})_2\text{L}^{\text{i-Pr}}$ .

(b) IR measurements. The IR spectra of polycrystalline powders were recorded within 4000–550  $\text{cm}^{-1}$  (mid-IR) at  $T=5\text{-}300$  K using FTIR spectrometer Bruker Vertex 80v (Bruker Optics, Germany) equipped with continuous flow liquid He cryostat Oxford OptistatCF. Infrared microscope HYPERION 2000 (Bruker Optics, Germany) equipped with sample stage Linkam FTIR600 (Linkam Scientific Instruments, United Kingdom) was used for measurements on single crystals at  $T=80$  and 300 K. Spectral resolution was 2  $\text{cm}^{-1}$ . The samples were thermally equilibrated during 5 min for each temperature-dependent measurement.

(c) Irradiation conditions. Steady-state halogen white light source was used in LIESST experiments with average power ≈20 mW/cm<sup>2</sup>. White light was applied perpendicular to the scanning IR irradiation, and the surface of pellet was inclined by 45° with respect to the scanning light to allow both irradiations simultaneously. The typical time of irradiation was ~10 minutes; after this time no significant spectral changes were observed.

## II. MANIFESTATION OF LIGHT AND THERMALLY-INDUCED STRUCTURAL CHANGES IN FTIR SPECTRA OF $\text{Cu}(\text{hfac})_2^{\text{R}}$

Figure 3 of the main text shows FTIR spectra of  $\text{Cu}(\text{hfac})_2\text{L}^{\text{Me}}$  and  $\text{Cu}(\text{hfac})_2\text{L}^{\text{Pr}}$  in thermal SS, WS and photoinduced mWS states in the most informative mid-IR range 1100–800  $\text{cm}^{-1}$ . Here we would like to present the full-range mid-IR spectra, which reproduce the trends described in the main text.

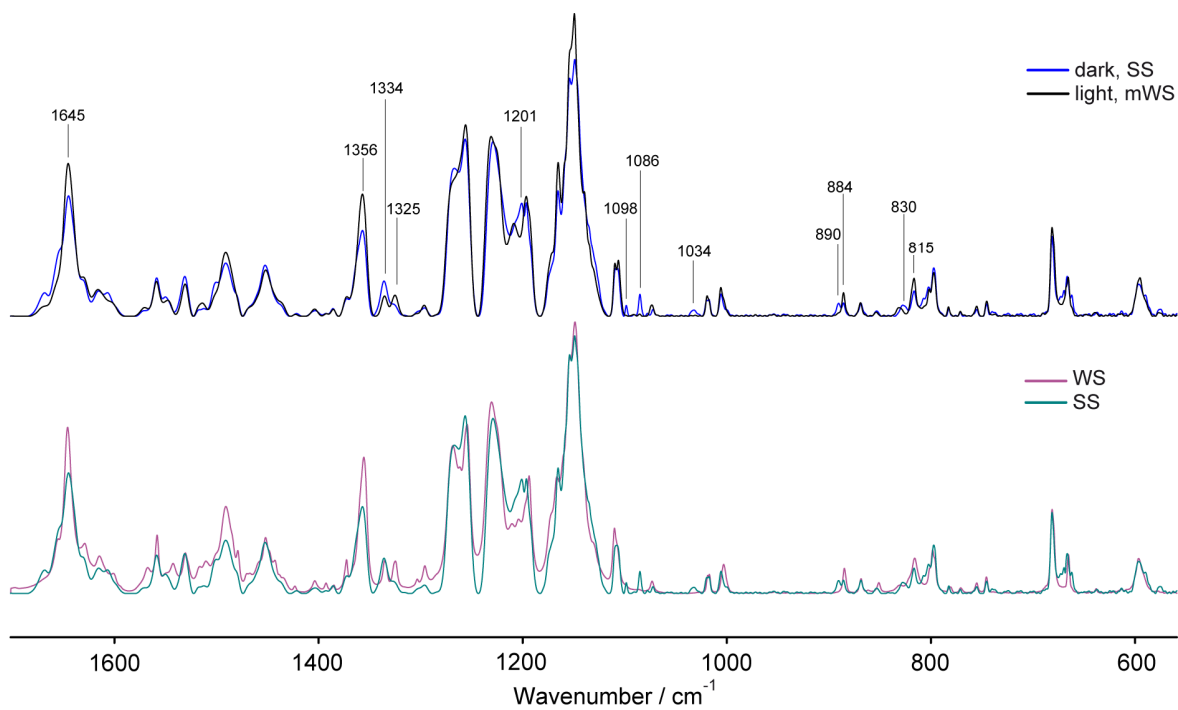


**Figure S1.** Mid range FTIR absorbance spectra of  $\text{Cu}(\text{hfac})_2\text{L}^{\text{Me}}$  in temperature-induced WS state (purple, 150 K), light-induced mWS state (black, 5 K), SS spin state at 25 K (blue (top) and turquoise (bottom)).

The similarity of crystal structures of WS and mWS states in  $\text{Cu}(\text{hfac})_2\text{L}^{\text{Me}}$  is confirmed by the coincidence of the FTIR spectra in a whole mid-IR range: under light irradiation all vibrational bands characteristic for SS state disappear ( $1334, 1201, 1098, 1086, 1034, 890 \text{ cm}^{-1}$ ), and vibrational bands characteristic for WS state grow in intensity ( $1645, 1356, 1325, 884, 815 \text{ cm}^{-1}$ ).

In case of the second compound  $\text{Cu}(\text{hfac})_2\text{L}^{\text{Pr}}$  we observe similar trend. White light irradiation results in intensity decrease of characteristic vibrational bands for SS state ( $1649, 1553, 1504, 1193, 1139, 1092, 893, 793$  and  $672 \text{ cm}^{-1}$ ) and intensity increase of characteristic vibrational bands for WS state ( $1641, 1558, 1355, 1105$  and  $798 \text{ cm}^{-1}$ ). This indicates general similarity of structures of mWS and WS states. Nevertheless, as was already mentioned in the main text, some characteristic IR bands that change during SS $\rightarrow$ WS conversion are not sensitive to light-induced SS $\rightarrow$ mWS conversion. The intensity of bands at  $1039$  and  $904 \text{ cm}^{-1}$  remains the same during light irradiation, whereas it undergoes appreciable changes during temperature variation from 25 to 300 K. This fact indicates structural differences of thermal WS and light-induced mWS states in  $\text{Cu}(\text{hfac})_2\text{L}^{\text{Pr}}$  assigned to different conformations of peripheral propyl groups of nitroxide radical. As was shown by XRD analysis, thermal WS and SS states of  $\text{Cu}(\text{hfac})_2\text{L}^{\text{Pr}}$  have different orientation of propyl substituent in nitroxide radical (see main text), and in process of

fast light-induced switching the orientation of propyl group does not change as it does during slow thermal transition.

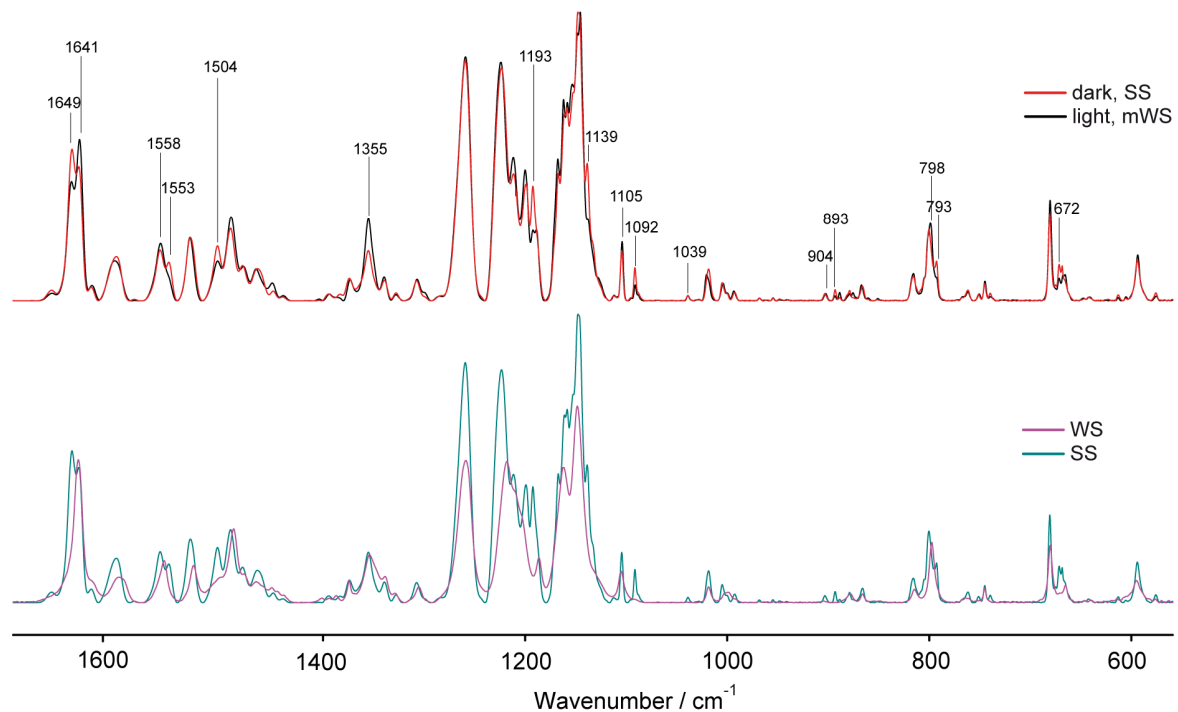


**Figure S2.** Mid range FTIR absorbance spectra of  $\text{Cu}(\text{hfac})_2\text{L}^{\text{Pr}}$  in temperature-induced WS state (purple, 300 K), light-induced mWS state (black, 5 K), SS spin state (red (top) and turquoise (bottom), 25 K).

The assignment of thermo-sensitive but light-insensitive vibration bands to propyl groups was additionally supported by comparison with the sister compound  $\text{Cu}(\text{hfac})_2\text{L}^{\text{i-Pr}}$  (see main text). Similar to  $\text{Cu}(\text{hfac})_2\text{L}^{\text{Pr}}$ , the complex  $\text{Cu}(\text{hfac})_2\text{L}^{\text{i-Pr}}$  demonstrates the ability for light-induced switching, during which all vibrational bands characteristic for SS state ( $1090, 1018, 1004, 885, 865 \text{ cm}^{-1}$ ) decrease in intensity, and characteristic vibrational bands of WS state ( $1105, 881 \text{ cm}^{-1}$ ) increase in intensity.

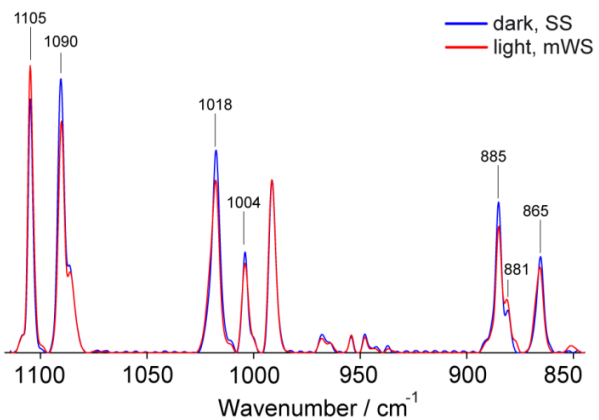


**Figure S3.** Mid range FTIR absorbance spectra of  $\text{Cu}(\text{hfac})_2\text{L}^{\text{i-Pr}}$  in light-induced mWS state (red, 5 K) and SS spin state (blue, 25 K).

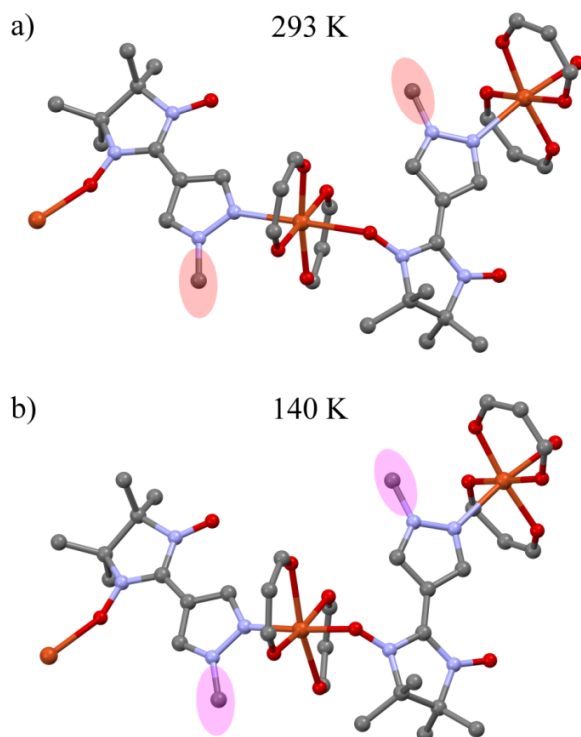


**Figure S4.** The structure of  $\text{Cu}(\text{hfac})_2\text{L}^{\text{Me}}$  with head-to-tail coordination at temperatures above (293 K) and below (140 K) magneto-structural transition. Alkyl substituent of nitroxide radical is highlighted by corresponding colors.

In case of complex  $\text{Cu}(\text{hfac})_2\text{L}^{\text{Me}}$ , no structural changes in conformation of nitroxide ligand are found during thermal transition. All changes occurs in  $\text{CuO}_5\text{N}$  unit (see Figure S4), and therefore

the structure of light-induced mWS state perfectly corresponds to the structure of thermal WS state.

### III. RELAXATION PROPERTIES OF LIGHT-INDUCED SPIN STATE

Maximum photoconversion efficiency ( $\gamma_{\max}$ ) and mWS $\rightarrow$ SS relaxation time ( $\tau$ ) of the photoinduced state are important parameters in LIESST studies, because, in particular, they carry information on the activation energy barrier ( $E_A$ ).<sup>S4</sup> In this work we did not study these parameters in detail and did not investigate their temperature dependence, but still we performed comparison for Cu(hfac)<sub>2</sub>L<sup>Me</sup> and Cu(hfac)<sub>2</sub>L<sup>Pr</sup> in particular conditions.

To monitor the SS $\rightarrow$ mWS conversion and to estimate the mWS/SS ratio ( $\gamma$ ) we have selected characteristic and well resolved vibrational bands, which have been previously used to study thermally-induced SS $\rightarrow$ WS conversion:<sup>S8</sup> (i) two bands with maxima at 884 cm<sup>-1</sup> (WS) and 890 cm<sup>-1</sup> (SS) for Cu(hfac)<sub>2</sub>L<sup>Me</sup> compound; and (ii) two bands with maxima at 1105 cm<sup>-1</sup> (WS) and 1092 cm<sup>-1</sup> (SS) for Cu(hfac)<sub>2</sub>L<sup>Pr</sup> compound.

Recorded under the steady-state irradiation,  $\gamma_{\max}(T)$  function allows determining maximum photo-induced conversion that can be reached for particular sample. As one can see from Figure S5a, the SS $\rightarrow$ mWS conversion for Cu(hfac)<sub>2</sub>L<sup>Me</sup> compound begins already at 25 K and almost reaches its plateau at 10 K. In case of Cu(hfac)<sub>2</sub>L<sup>Pr</sup> compound the light-induced SS $\rightarrow$ mWS conversion begins at 20 K and the plateau is expected at  $T < 5$  K. Thus, the structural investigation of light-induced mWS state should be performed at minimum temperature available (5 K in our case). At the same time, FTIR spectra of SS states should be measured at  $T=25$  K (above LIESST region) in order to avoid any possible contribution of photoswitched clusters.

We reliably established that  $\gamma_{\max}(T)$  dependence for Cu(hfac)<sub>2</sub>L<sup>Pr</sup> decays faster with temperature compared to that for Cu(hfac)<sub>2</sub>L<sup>Me</sup> (Figure S5a), so the whole curve is shifted to the lower temperatures by approx. 5 K. The possible reason for such effect is the difference in activation energy  $E_A$  between SS and mWS states, and for the Cu(hfac)<sub>2</sub>L<sup>Me</sup> compound  $E_A$  is expected to be larger than for Cu(hfac)<sub>2</sub>L<sup>Pr</sup>. Indeed, mWS state of Cu(hfac)<sub>2</sub>L<sup>Me</sup> compound shows better stability in terms of mWS $\rightarrow$ SS relaxation (see Figure S5b): the mWS state of Cu(hfac)<sub>2</sub>L<sup>Me</sup> almost does not relax within first hour, whereas in case of Cu(hfac)<sub>2</sub>L<sup>Pr</sup> approx. 20% of initial mWS states relaxed back to SS state. These facts, as well as temperatures of magneto-structural transition for both compounds (Cu(hfac)<sub>2</sub>L<sup>Me</sup> – 146 K, Cu(hfac)<sub>2</sub>L<sup>Pr</sup> –  $\sim$ 200

K), are in good agreement with the Buhks theory theses: the tunneling rate is faster for larger energy difference between the SS and WS states ( $\Delta E_0$ ); the larger  $\Delta E_0$ , the higher is the temperature of the thermally-induced spin transition.<sup>S9</sup>

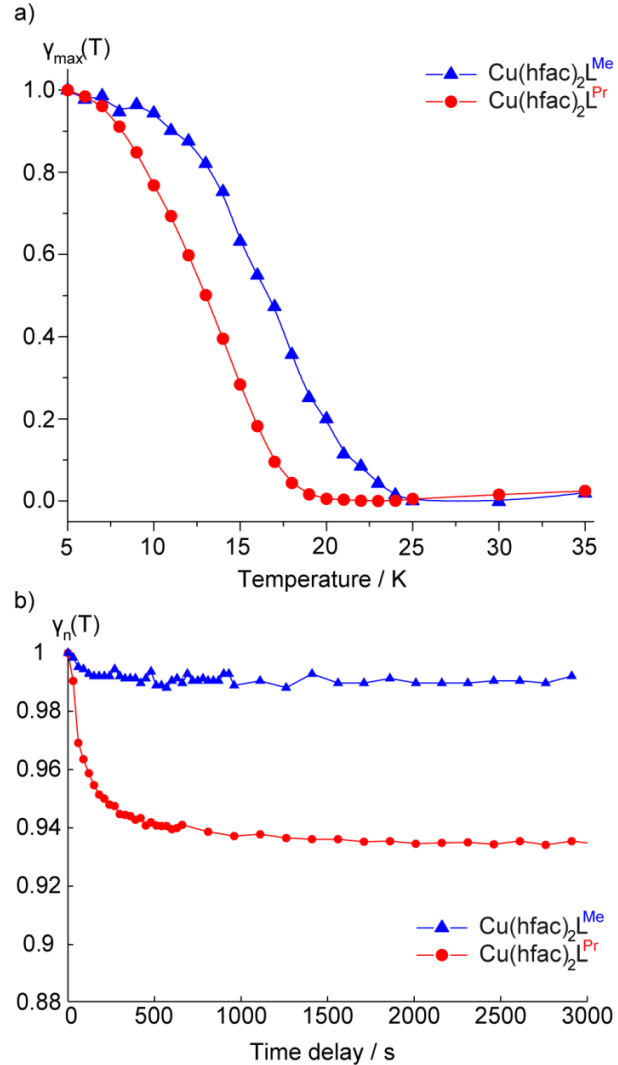


**Figure S5.** a) Maximum conversion depth  $\gamma_{\max}=\gamma_n(t=0)$  vs. temperature for  $\text{Cu}(\text{hfac})_2\text{L}^{\text{Me}}$  and  $\text{Cu}(\text{hfac})_2\text{L}^{\text{Pr}}$ . The curves are normalized to  $\gamma_{\max}(5 \text{ K})$ . b) Normalized relaxation dependences  $\gamma_n(t)$  measured for  $\text{Cu}(\text{hfac})_2\text{L}^{\text{Me}}$  and  $\text{Cu}(\text{hfac})_2\text{L}^{\text{Pr}}$  at 5 K.

We also compared  $\gamma_{\max}(T)$  behavior for  $\text{Cu}(\text{hfac})_2\text{L}^{\text{Pr}}$  in KBr with previously obtained results for  $\text{Cu}(\text{hfac})_2\text{L}^{\text{Pr}}$  mixed with glycerol (Figure S6).<sup>S4</sup> Surprisingly, in spite of principally different methods of sample preparation, the curves are very similar. The minor difference at lowest temperatures (5-9 K) might be explained by small uncertainty of sample temperature measurement in the cryostat of FTIR spectrometer.

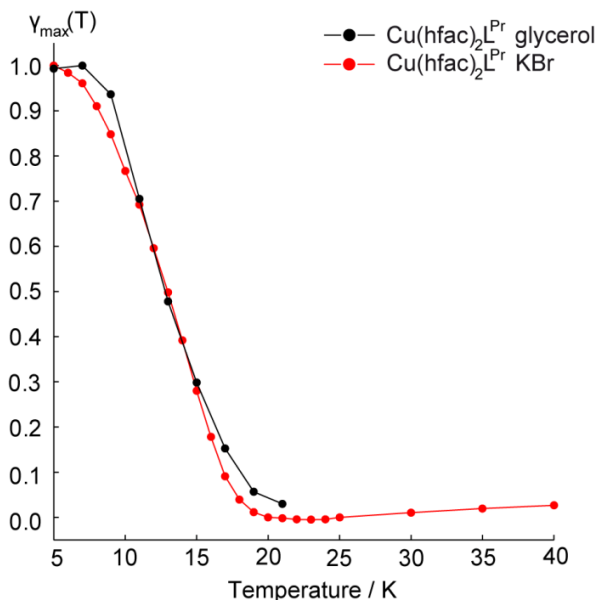


**Figure S6.** a) Maximum conversion depth  $\gamma_{\max} = \gamma_n(t=0)$  vs. temperature for  $\text{Cu}(\text{hfac})_2\text{L}^{\text{Pr}}$  mixture with glycerol (black)<sup>S4</sup> and compressed in KBr pellet (red). The curves are normalized to  $\gamma_{\max}(5 \text{ K})$ .

## REFERENCES

- S1. V. I. Ovcharenko, S. V. Fokin, G. V. Romanenko, Y. G. Shvedenkov, V. N. Ikorskii, E. V. Tretyakov and S. F. Vasilevskii, *J. Struct. Chem.*, 2002, **43**, 153-167.
- S2. V. I. Ovcharenko, K. Y. Maryunina, S. V. Fokin, E. V. Tretyakov, G. V. Romanenko, V. N. Ikorskii, *Russ. Chem. Bull.*, 2004, **53**, 2406-2427.
- S3. M. V. Fedin, E. G. Bagryanskaya, H. Matsuoka, S. Yamauchi, S. L. Veber, K. Y. Maryunina, E. V. Tretyakov, V. I. Ovcharenko and R. Z. Sagdeev, *J. Am. Chem. Soc.*, 2012, **134**, 16319-16326.
- S4. M. V. Fedin, K. Y. Maryunina, R. Z. Sagdeev, V. I. Ovcharenko and E. G. Bagryanskaya, *Inorg. Chem.*, 2012, **51**, 709-717.
- S5. I. Y. Barskaya, E. V. Tretyakov, R. Z. Sagdeev, V. I. Ovcharenko, E. G. Bagryanskaya, K. Y. Maryunina, T. Takui, K. Sato and M. V. Fedin, *J. Am. Chem. Soc.*, 2014, **136**, 10132-10138.
- S6. W. Kaszub, A. Marino, M. Lorenc, E. Collet, E. G. Bagryanskaya, E. V. Tretyakov, V. I. Ovcharenko and M. V. Fedin, *Angew. Chem.-Int. Edit.*, 2014, **53**, 10636-10640.
- S7. M. V. Fedin, S. L. Veber, E. G. Bagryanskaya and V. I. Ovcharenko, *Coord. Chem. Rev.*, 2015, **289–290**, 341-356.

S8. S. L. Veber, E. A. Suturina, M. V. Fedin, K. N. Boldyrev, K. Y. Maryunina, R. Z. Sagdeev, V. I. Ovcharenko, N. P. Gritsan and E. G. Bagryanskaya, *Inorg. Chem.*, 2015, **54**, 3446-3455.

S9. E. Buhks, G. Navon, M. Bixon, J. Jortner, *J. Am. Chem. Soc.*, 1980, **102**, 2918-2923.